

PFC/JA-92-18

Time Dependent Effects of  
Fusion Reactivity Enhancement due to Minority  
Heating in D-T and D-<sup>3</sup>He Tokamak Plasmas

E. A. Chaniotakis  
D. J. Sigmar

June 1992

Plasma Fusion Center  
Massachusetts Institute of Technology  
Cambridge, Massachusetts 02139 USA

Submitted for publication in: *Nuclear Fusion*

This work was supported by DOE grant DE-FG02-91ER-54109.

# Time Dependent Effects of Fusion Reactivity Enhancement due to Minority Heating in D-T and D-<sup>3</sup>He Tokamak Plasmas

E.A. Chaniotakis, D.J. Sigmar

Plasma Fusion Center  
Massachusetts Institute of Technology

## ABSTRACT

*In D-T and D-<sup>3</sup>He plasmas ICRF heating at the second harmonic of deuterium results in the modification of the distribution function of the heated ions. This paper describes such effects on the dynamic behavior of plasmas. Using a 0-D plasma transport model the effect of ICRF heating on the plasma operating contours is analyzed for the ITER, and a D-<sup>3</sup>He tokamak. To describe the dynamic behavior, a model for the characteristic time of tail relaxation,  $\tau_\xi$ , is developed and a feedback model based on auxiliary power is presented. The stabilization of temperature perturbations in a D-<sup>3</sup>He plasma is simulated for various values of  $\tau_\xi$ .*

## 1 Introduction

As the world fusion program is approaching the burning plasma state there is increasing interest in understanding plasma operating point control and thermal instability. Strong auxiliary heating power  $P_{aux}$  is required to cross the Cordey pass and if ICRH is used – the ensuing energetic minority ion tail will affect the fusion reactivity and hence the burn dynamics, particularly if the main burn control system relies on tailoring  $P_{aux}$  dynamically in response to thermal excursions.

Dawson, Furth and Tunney [1] were the first to point out the fusion reactivity enhancement due to auxiliary (N.B.I.) heating. Later, following

the ground breaking work of Stix [2] on ion tail formation due to ICRH, Kesner [3] performed an investigation of the combined effect of NBI and ICRH driven fuel ion distribution function distortions on the thermonuclear energy multiplication factor  $Q$ . Blackfield and Scharer [4] applied a 2-D (in velocity space), 0-D (in configuration space) Fokker-Planck ICRF code to (PLT and) the hypothetical NUWMAK tokamak reactor and found little  $Q$  enhancement due to deuteron minority heating for their parameter regime. Later, Scharer et. al. [5] performed a specific analysis for JET with fundamental deuteron minority heating in a tritium plasma resulting in a 1.6 – 1.9 fusion power enhancement after a 1 sec heating pulse.

Using their bounce averaged Fokker-Planck quasilinear code, Harvey et. al. [6] analyzed second harmonic heating of a 50:50 D-T plasma. Depending on the chosen density, the ion tail can be pushed out beyond the maximum of the D-T  $\langle\sigma_f v\rangle$  curve. At values of  $Q < 1$  sizable ion tail driven enhancement factors of the reactivity can be obtained but at  $Q > 1$  the enhancement decreases rapidly in this ICRF heating scenario.

Returning to minority heated fusion plasma scenarios, we focus in the present work on a different novel aspect, i.e. the problem of operating point control in tokamaks relying on variable ICRF heating for burn control. Besides burn control it appears that the resulting phase lag of the plasma temperature time response can yield important information on energy equilibration and confinement time of the main ions, the minority and the fusion products.

In Section 2 after briefly recasting the Stix formula for the energetic ion tail driven by ICRH, we pursue its consequences for the fusion reactivity  $\langle\sigma_f v\rangle$  averaged over a fuel ion distribution function with effective temperature  $T_{eff} = T/\mathcal{F}(\xi)$  where  $\xi \propto P_{icrh}\sqrt{T_e}/n_e^2$  is the Stix parameter and  $\mathcal{F}$  is a known function. In Section 3 we implement the ICRH enhanced fusion power source term in the 0-D plasma power balance in a space spanned by plasma density and temperature and analyze the self-consistent (nonlinear

in  $P_{icrh}$ ) steady state solutions of the plasma power balance for (a) ITER and (b) a 10 Tesla,  $R_0 = 6.3$  m, D-<sup>3</sup>He advanced reactor design. In Section 4, the 0-D steady state power balance of Section 3 is extended to the time dependent case to study the dynamic effects of the energetic ion tail equilibration with the bulk plasma and its implications for operating point control using a simple feedback law but including the delayed additional heating power input from the ICRH minority tail. Sections 5 contains a summary and conclusions.

## 2 Distribution function modifications due to ICRH

Before the distribution function, rederived in Appendix A, is used to calculate the fusion reactivity and the plasma performance it is useful to investigate the effect of the various plasma parameters on the shape of the distribution function. It is shown in Appendix A that the parameter  $\xi$  depends on the applied ICRF power density, ( $P_{ICRF}$ ), and on the plasma density and temperature, i.e.

$$\xi = \xi (\langle P_{ICRF} \rangle, T, n), \quad (1)$$

namely (from Eq.(45) in Appendix A),  $\xi$  follows the scaling,

$$\xi \sim \frac{\langle P_{ICRF} \rangle T_e^{1/2}}{n_e^2}, \quad (2)$$

As  $\xi$  increases, the distribution function deviates increasingly from the Maxwellian. The deviation becomes pronounced for  $\xi \geq 1$ , and thus it is important to determine the values of the density, temperature and ICRF heating power density that result in  $\xi = 1$ . The relation between  $\xi$ ,  $n$ ,  $T$ , and  $\langle P_{ICRF} \rangle$  is shown in Fig. 1 where the  $\xi = 1$  contour is shown in the density-temperature operating space for a D-T plasma for various values of  $\langle P_{ICRF} \rangle$ .

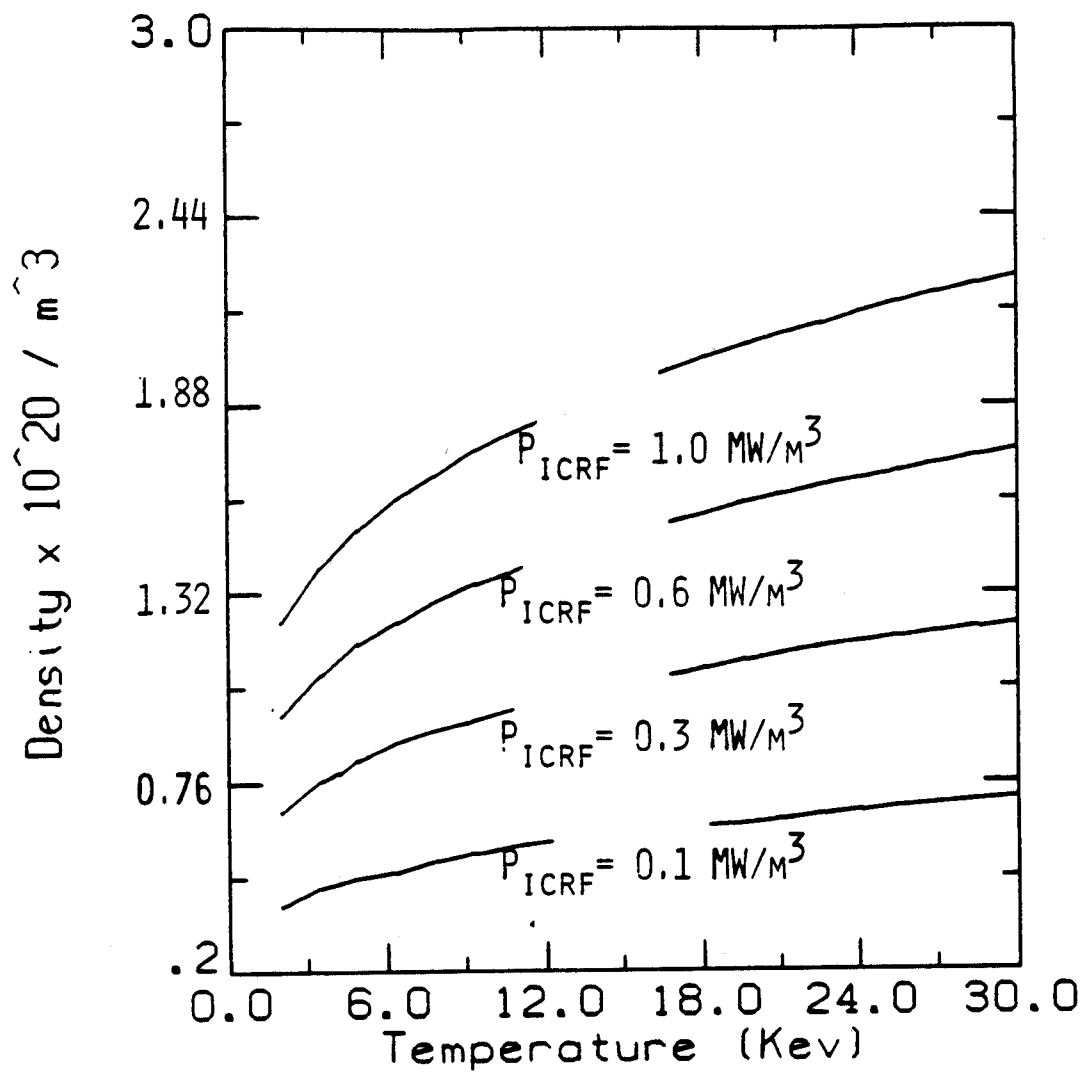


Figure 1: The contours  $\xi = 1$  for the various values of ICRF heating power density indicated on each contour.

Two contours on Fig. 1 are of significant importance. The contour labeled  $0.1 \text{ MW/m}^3$  corresponds approximately to the power density for the technology phase of the ITER tokamak, and the contour labeled  $0.6 \text{ MW/m}^3$  corresponds to the power density of a high field, CIT like, tokamak. Note that as the power density increases the  $\xi = 1$  contour encompasses more of the density - temperature operating space.

As an example of the change in the distribution function of ions heated by ICRF, a D-<sup>3</sup>He plasma is considered with the following parameters.

Electron density	$n_e = 0.7 \times 10^{20}/\text{m}^3$	
Deuterium density	$n_D = \frac{1}{3}0.7 \times 10^{20}/\text{m}^3$	
Tritium density	$n_T = \frac{1}{3}0.7 \times 10^{20}/\text{m}^3$	(3)
Electron temperature	$T_e = 50\text{keV}$	
Heating power	$\langle P_{\text{ICRF}} \rangle = 0.11\text{MW}/\text{m}^3$	

The value of the parameter  $\xi$  is a function of the electron temperature and the dependance is shown in Fig. 2. Note that  $\xi$  increases with temperature as indicated by Eq. 45. For reference, a plot of the function  $H$ , given by Eq. 48, is also shown on Fig. 2.[2]

For the plasma parameters indicated above the distribution function of the heated deuterium ions is shown on Fig. 3. The dotted line represents the distribution due to ICRF heating and the solid line corresponds to a Maxwellian distribution. The change in the distribution function due to ICRF, for the D-<sup>3</sup>He plasma under investigation, is significant for this case.

## 2.1 Effect of ICRF heating on the fusion reaction rate

In the previous section the change in the distribution function of ICRF heated ions was shown to be significant under certain circumstances when

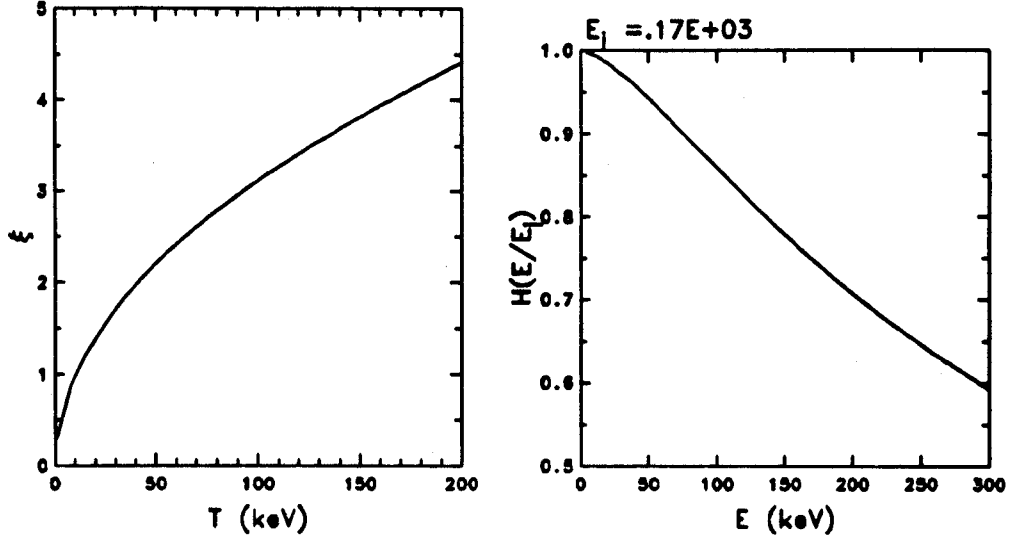


Figure 2: Left: The parameter  $\xi$  as a function of plasma background temperature for a D-<sup>3</sup>He plasma heated by .11 MW/m<sup>3</sup> of ICRF power. The density of the deuterium and tritium ions is  $0.23 \times 10^{20}/\text{m}^3$ . Right: The function  $H$  (see Eq. 48) for a D - <sup>3</sup>He plasma as a function of the energy of the resonant ions for  $\xi = 2.2$ .

compared with the equivalent Maxwellian distribution function. This change in the distribution function results in changes in the fusion reactivity  $\langle\sigma v\rangle$  affecting the fusion reaction rate and thus the overall plasma power balance.

The reaction rate,  $R$ , of a thermonuclear plasma depends on the reactivity of the interacting particles and on their density. For a plasma composed of two species with density  $n_1$  and  $n_2$  the reaction rate is given by

$$R_{12} = n_1 n_2 \langle\sigma v\rangle \quad (4)$$

The reactivity  $\langle\sigma v\rangle$  is given by

$$\langle\sigma v\rangle = \frac{4}{\sqrt{2\pi m_1}} \left(\frac{m_r}{m_1 T}\right)^{3/2} \int_0^\infty \exp\left[\left(-\frac{m_r E}{m_1 T}\right) \mathcal{F}(\xi)\right] E \sigma(E) dE \quad (5)$$

In the above equation  $m_r = m_1 m_2 / (m_1 + m_2)$  is the reduced mass of the reacting particles and  $T$  is the temperature of the background ions. For a plasma whose species are characterized by Maxwellian distributions the

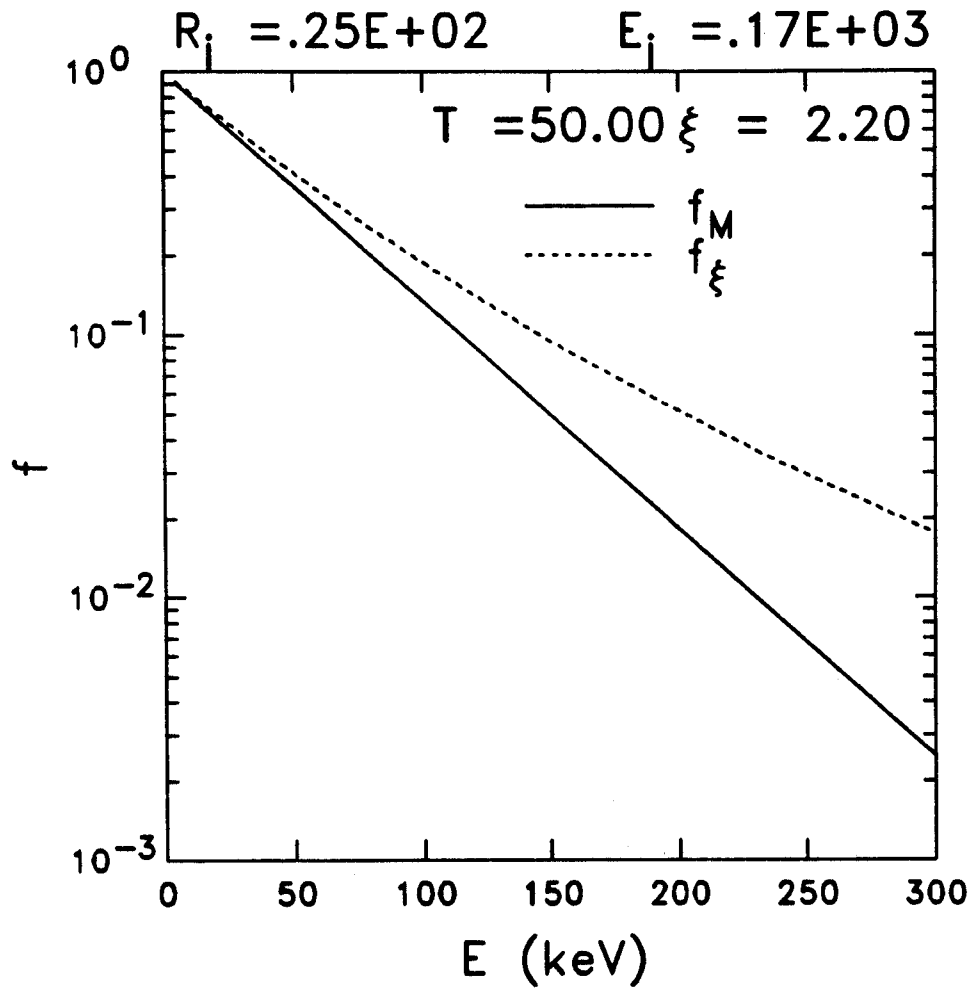


Figure 3: Normalized distribution function of Maxwellian (solid line) and ICRF heated deuterium ions in a D-<sup>3</sup>He plasma with an assumed background temperature of 50 keV. The ICRF power density is .11 MW/m<sup>3</sup> and the density of the deuterium and tritium ions is  $0.23 \times 10^{20}/\text{m}^3$ . Expressions for the parameters  $R_j$  and  $E_j$  are given by Eqs. 46 and 47 respectively.



function  $\mathcal{F}(\xi)$  is equal to unity. However, for ICRF heated plasmas the function  $\mathcal{F} < 1$  and thus the resulting reactivity differs from the reactivity of pure Maxwellian plasmas.

Once the cross section,  $\sigma$ , of the reaction is characterized, Eq. (5) determines the reactivity. In this analysis the reactivity of D-T and D-<sup>3</sup>He plasmas is evaluated by using the cross section fits of Sadler[7] and Peres[8].

For Maxwellian plasmas the reactivity  $\langle\sigma v\rangle$  is independent of the plasma density, but for ICRF heated plasmas the function  $\mathcal{F}$ , and thus the reactivity, depend on the plasma density (cf. Eq. (42)). The following examples are considered:

D-T Plasma	D- <sup>3</sup> He Plasma	
$n_e = 0.7 \times 10^{20}/m^3$	$n_e = 0.7 \times 10^{20}/m^3$	
$n_D = \frac{0.7}{2} \times 10^{20}/m^3$	$n_D = \frac{0.7}{3} \times 10^{20}/m^3$	(6)
$n_T = \frac{0.7}{2} \times 10^{20}/m^3$	$n_{^3He} = \frac{0.7}{3} \times 10^{20}/m^3$	
$\langle P_{ICRF} \rangle = 0.11 \text{ MW}/m^3$	$\langle P_{ICRF} \rangle = 0.11 \text{ MW}/m^3$	

In Fig. 4 the reactivity of the D-T plasma, whose parameters are given in (6), is shown for the cases when both the deuterium and tritium ions are characterized by a Maxwellian distribution, and when the deuterium ions are heated by 0.11 MW/m<sup>3</sup> of ICRF waves. A similar plot for the reactivity of a D-<sup>3</sup>He plasma is shown on Fig. 5.

### 3 Steady state issues: Operating point selection including ICRF produced ion tail

In the analysis that follows the performance of tokamak plasmas is investigated with the aide of a volume averaged (0-D) plasma transport model.

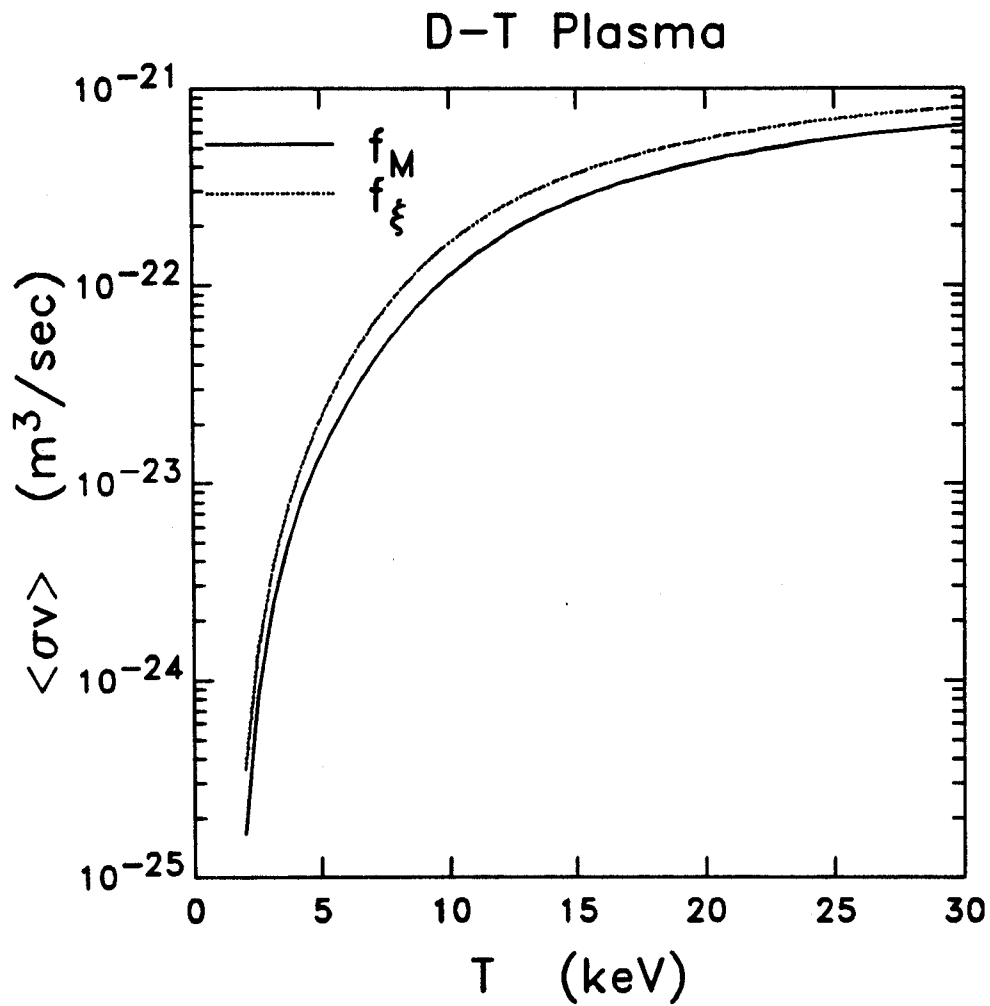


Figure 4: The reaction rate  $\langle \sigma v \rangle$  as a function of plasma temperature for a D-T plasma characterized by Maxwellian distribution functions (solid curve) and for a D-T plasma whose deuterium ions are heated by 0.11 MW/m<sup>3</sup> of ICRF power.

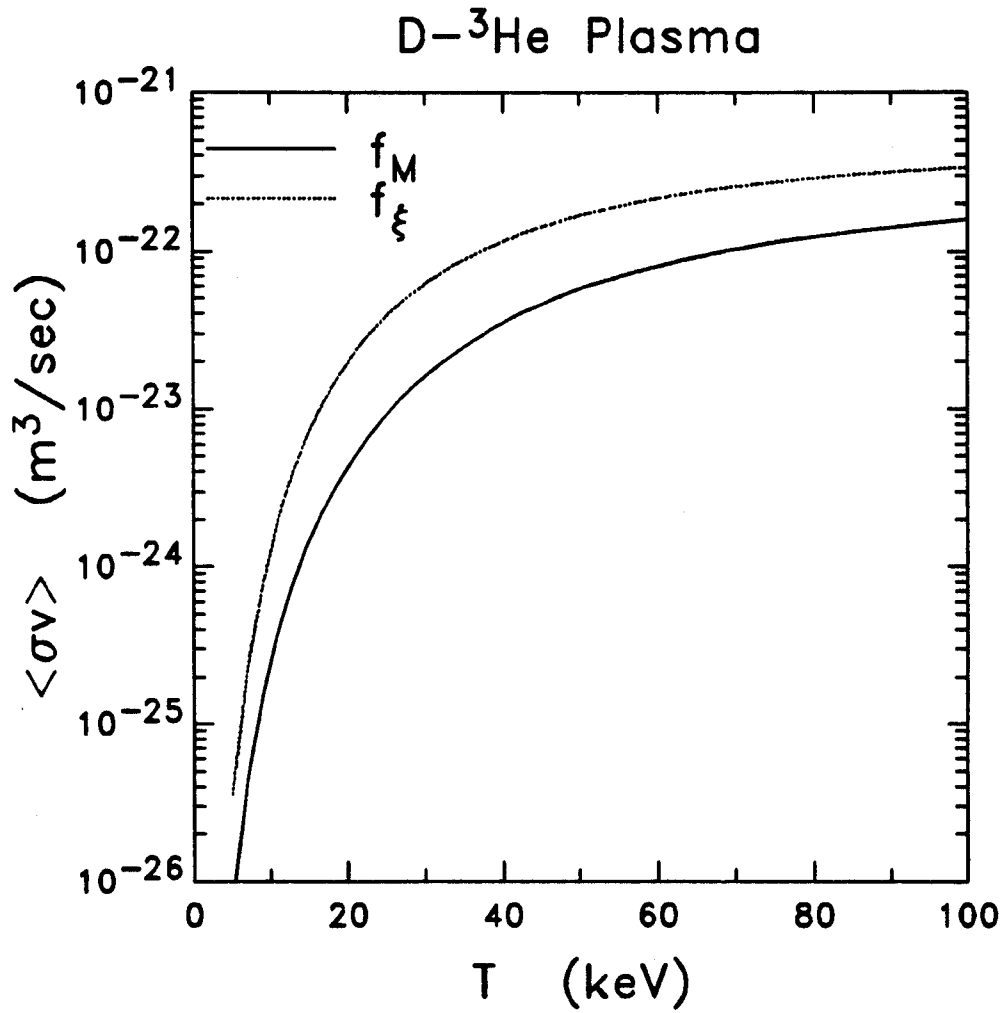


Figure 5: The reaction rate  $\langle \sigma v \rangle$  as a function of plasma temperature for a D-<sup>3</sup>He plasma characterized by Maxwellian distribution functions (solid curve) and for a D-<sup>3</sup>He plasma whose deuterium ions are heated by 0.11 MW/m<sup>3</sup> of ICRF power.

In such a model, the plasma density and temperature are characterized by fixed profile shapes and the averaging is performed over the plasma volume. In general the 0-D power balance of the ohmic  $P_\Omega$ , the fusion  $P_f$ , the auxiliary  $P_{aux}$ , the conduction losses  $P_l$ , the Bremsstrahlung radiation  $P_B$  and the synchrotron radiation  $P_s$  power densities, of a plasma with elliptic cross section, elongation  $\kappa$ , and with parabolic density and temperature profiles that are characterized by the exponents  $\nu_n$  and  $\nu_T$  respectively, are given by

$$\frac{0.024}{1 + \nu_n + \nu_T} (n_{e,0} + n_{i,0}) \frac{\partial T_0}{\partial t} = P_\Omega + \eta_f P_f + P_{aux} - P_l - P_B - P_s \quad (7)$$

With the temperature given in units of keV and the density in units of  $10^{20}/m^3$  the terms on the right hand side of Eq. 7 become

$$P_\Omega = 0.01045 \frac{\ln \Lambda Z_{eff}}{1 + 1.5\nu_T} \left( \frac{1 + \kappa^2}{\kappa} \right)^2 \frac{B_0^2}{R_0^2 T_{e0}^{3/2}} \quad (8)$$

$$P_l = \frac{0.024}{1 + \nu_n + \nu_T} \frac{(n_{e0} + n_{i0}) T_{e0}}{\tau_E} \quad (9)$$

$$P_B = \frac{.0053 Z_{eff}}{2\nu_n + 0.5\nu_T + 1} n_{e0}^2 T_{e0}^{1/2} \quad (10)$$

$$P_s \simeq 0.00621 \frac{n_{e0} T_{e0}}{1 + \nu_n + \nu_T} B_0^2 \left( 1 + \frac{T_{e0}}{146(1 + \nu_n + \nu_T)} \right) \quad (11)$$

where  $\ln \Lambda$ ,  $Z_{eff}$ ,  $B_0$ , and  $R_0$  are respectively the Coulomb logarithm, the effective charge, the magnetic field on axis, and the plasma major radius.

For a D-T plasma  $P_f$  corresponds to the alpha power  $P_\alpha$  which is given by

$$P_f \equiv P_\alpha = \frac{0.56}{\nu_T} n_{d,0} n_{t,0} F_f(T_0) \quad (12)$$

For a D-<sup>3</sup>He plasma the fusion power is given by

$$P_f = \frac{2.928}{\nu_T} n_{d,0} n_{^3\text{He},0} F_f(T_0) \quad (13)$$

The function  $F_f(T_0)$  is given by

$$F_f(T_0) = \frac{10^{22}}{T_0^{(2\nu_n+1)/\nu_T}} \int_0^{T_0} \sigma v(T) T^{(2\nu_n+1)/\nu_T-1} dT \quad (14)$$

The plasma self heating efficiency  $\eta_f$  allows for less than perfect coupling of the charged fusion product power  $P_f$  to the bulk plasma. In the present work it is assumed that  $\eta_f = 1$  throughout, although if  $\eta_f < 1$  can have important consequences in tokamak performance.[9]

The energy confinement time  $\tau_E$  is a combination between the ohmic (Neo-Alcator) [10] scaling  $\tau_{NA}$  and the auxiliary scaling  $\tau_{AU}$ . In this analysis the inverse quadrature form of Goldston is used for  $\tau_E$ .

$$\frac{1}{\tau_E} = \left( \frac{1}{\tau_{NA}^2} + \frac{1}{\tau_{AU}^2} \right)^{1/2} \quad (15)$$

The Neo-Alcator confinement scaling is given by

$$\tau_{NA} = 0.2 \bar{n}_e a R_0^2 \kappa^5 \quad (16)$$

In this analysis the auxiliary scaling is given by the ITER89P [11] energy confinement scaling

$$\tau_{AU} = 0.048 H \frac{I_P^{0.85} R_0^{1.2} a^{0.3} \kappa^{0.5} \bar{n}_e^{0.1} B_0^{0.2} A_i^{0.5}}{(P_{aux} + P_f)^{0.5}} \quad (17)$$

Here  $H$  represents the H-mode enhancement factor,  $I_P$  is the total plasma current in MA,  $a$  is the plasma minor radius,  $A_i$  is the average atomic mass number of the plasma ions, and  $P_{aux}$  is the auxiliary power in MW. For a D-T plasma  $P_f$  is the alpha power in MW and for a D-<sup>3</sup>He plasma  $P_f$  is the total fusion power in MW.

Table 1: Parameters for the Tokamaks under consideration

Parameters		ITER	D- <sup>3</sup> He
$R_0$	Major Radius (m)	6.0	6.3
$a$	Minor Radius (m)	2.15	2.0
$B_0$	Magnetic Field (T)	4.85	10
$I_P$	Plasma current (MA)	22	33
$H$	H-mode factor	1.85	4.0

By setting  $\partial T_0/\partial t = 0$  in Eq. 7 the effect of ICRF heating on plasma performance is investigated in the density-temperature operating space of the tokamaks whose parameters are given in Table 1.

By solving Eq. 7 for the auxiliary power in the density - temperature operating space we can obtain both the plasma operating contours (POP-CON) and the contours of constant  $\xi$  for the parameters given in Table 1. These contours are shown on Figs. 6, 7, 8, 9 for the ITER, and D-<sup>3</sup>He tokamaks.

Large values of  $\xi$  imply significant alteration of the resonant ions distribution function (see Eq. 42) which in turn results in appreciable changes in the fusion reactivity (reaction rate). In order to investigate the effect of ICRF tail heating “ $\xi$  effect” on machine performance we choose an operating point (density, temperature) and then calculate the auxiliary power required to sustain the operating point with and without the  $\xi$  effect.

In the ITER operating space (Fig. 6) the effect of  $\xi$  is calculated at the operating point  $n_{e_0} = 0.6 \times 10^{20}/\text{m}^3$ ,  $T_{e_0} = 32$  keV. In this case the auxiliary power required to maintain this operating point without the  $\xi$  effect is 16.5 MW and with the  $\xi$  effect the auxiliary power is reduced by 24% to 12.5 MW in steady state.

A similar analysis is performed for the D-<sup>3</sup>He tokamak. In the D-<sup>3</sup>He operating space we choose the operating point  $n_e = 1.0 \times 10^{20}/\text{m}^3$ ,  $T_e = 60$  keV. Sustaining operation at this point requires 36 MW of auxiliary power when no  $\xi$  effect is considered, and 28 MW with the inclusion of the  $\xi$  effect. This results in a 22% decrease in the required auxiliary power.

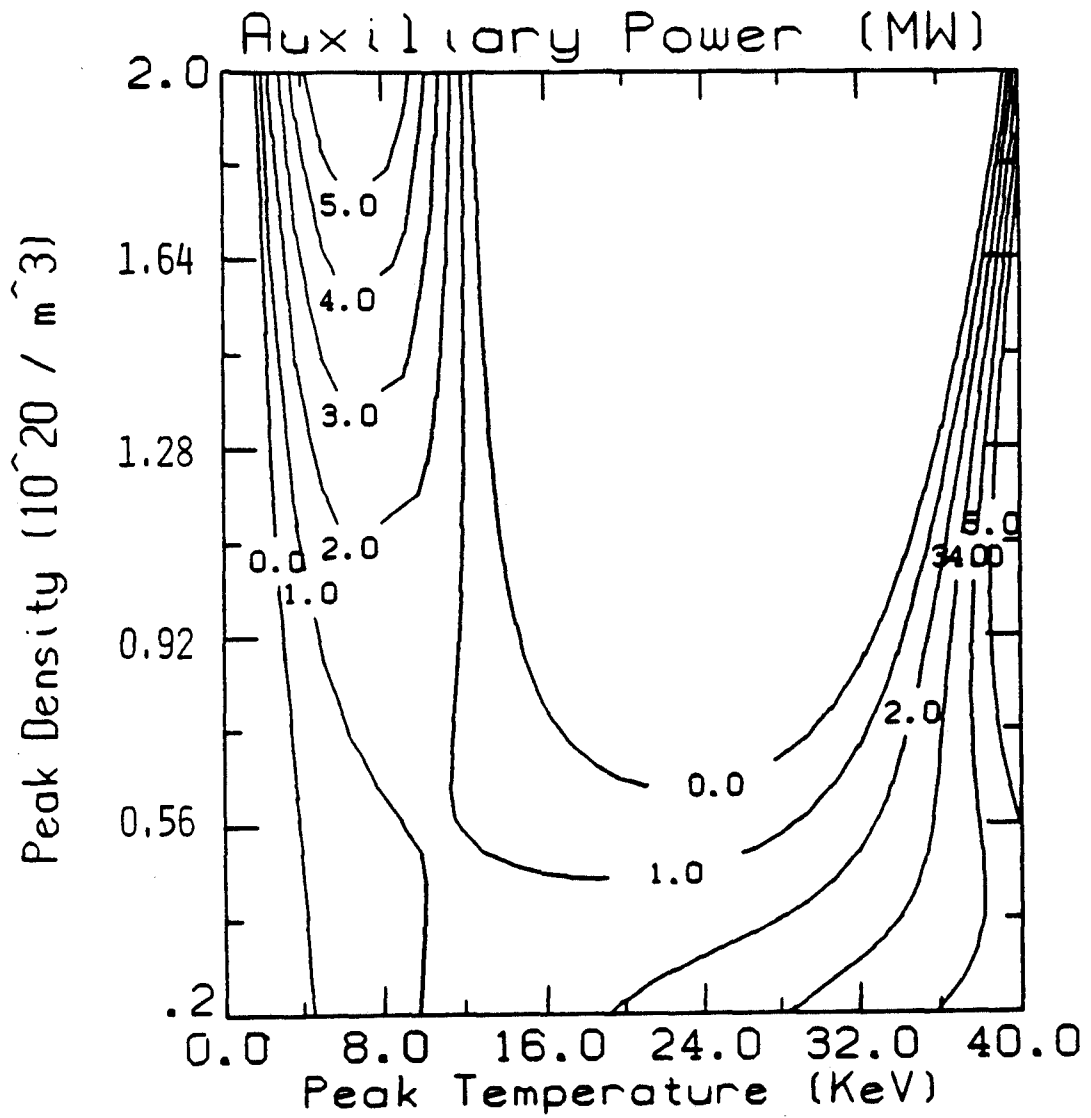


Figure 6: ITER density-temperature operating space with contours of auxiliary power in  $MW \times 10^3$ .

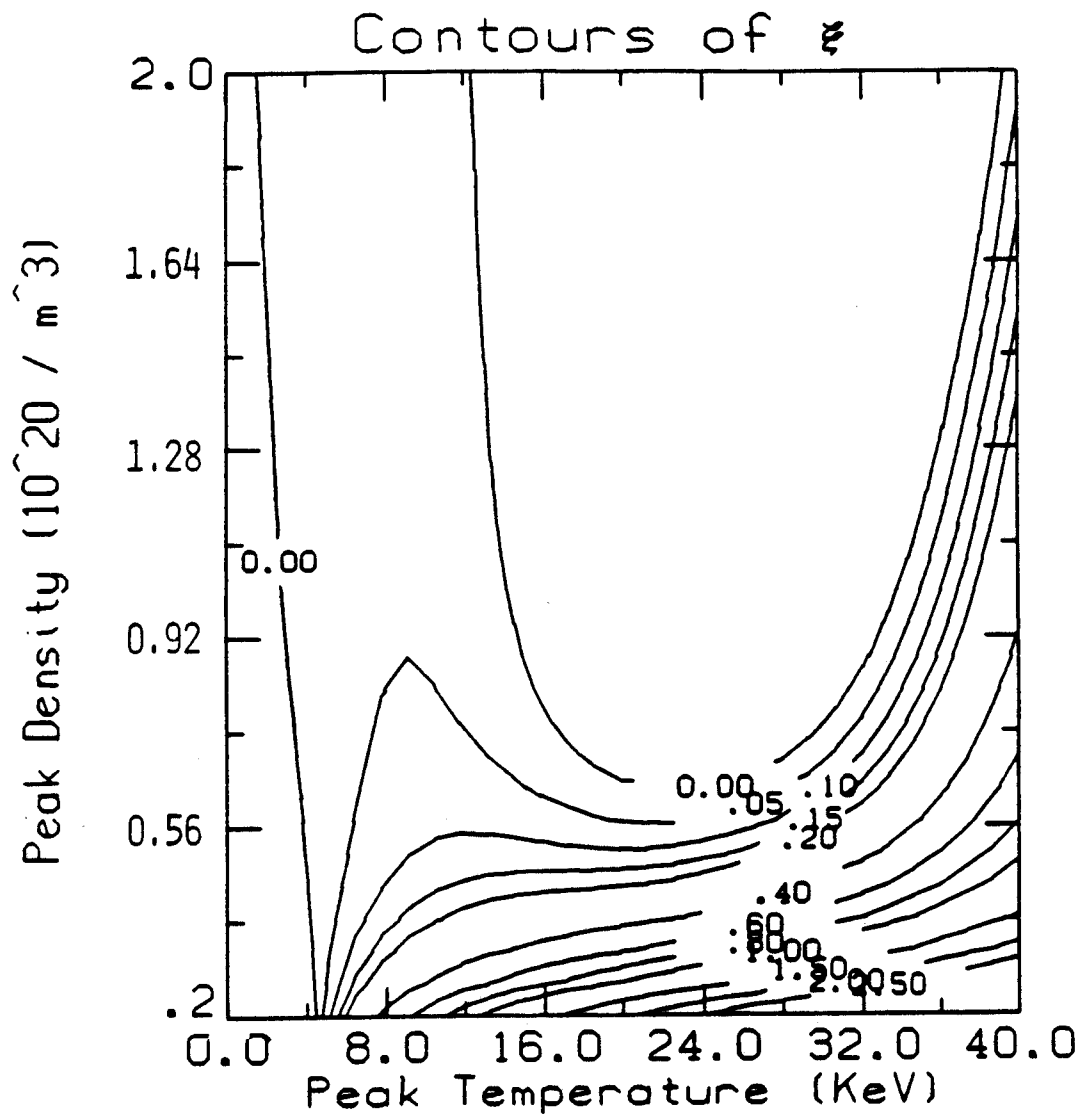


Figure 7: ITER contours of constant  $\xi$  (cf. Eq. 45) for D-T fusion. The  $P_{ICRF}$  values needed in evaluating  $\xi$  are taken from Fig. 6 at each value of density and temperature.



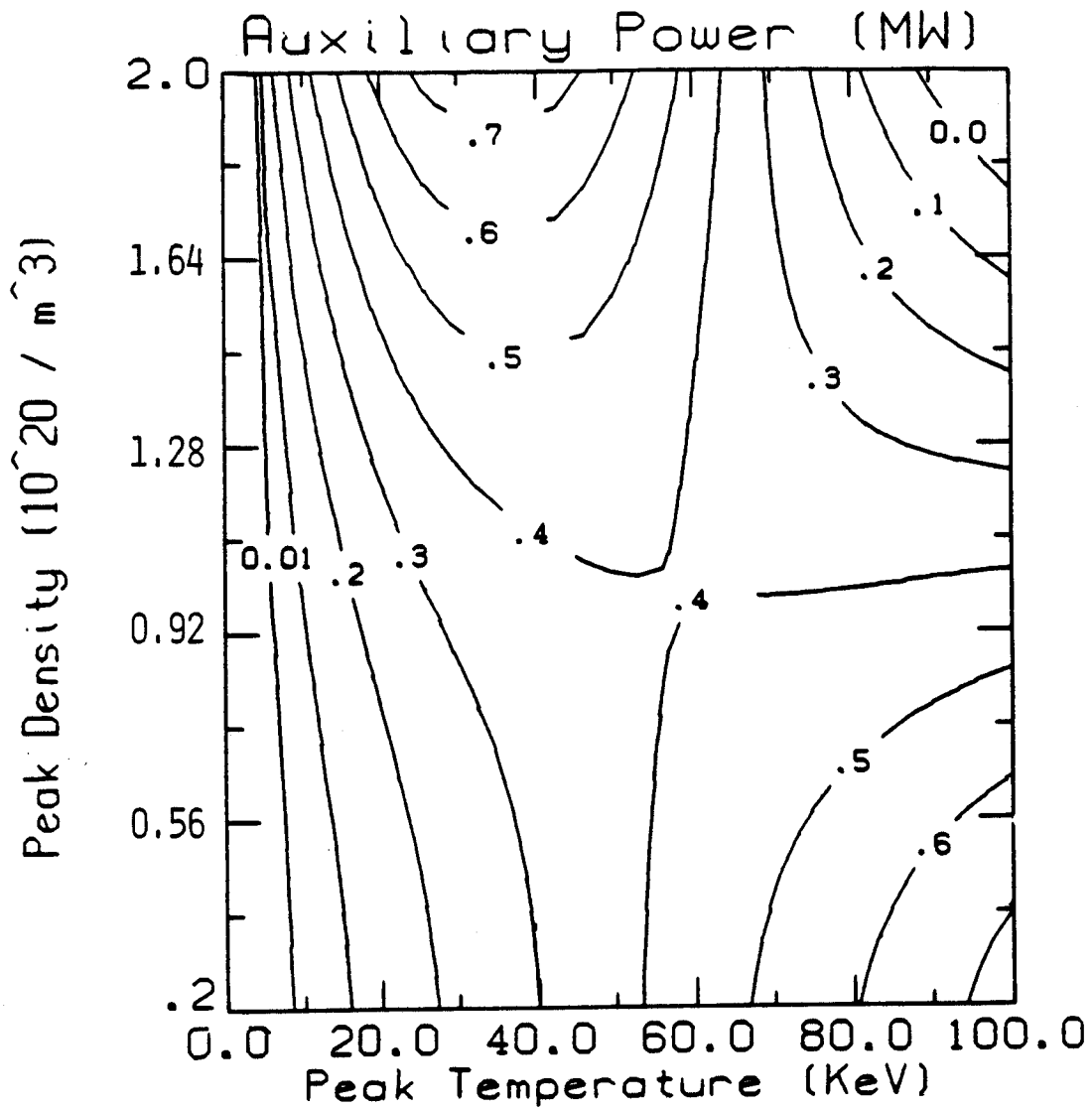


Figure 8: D-<sup>3</sup>He reactor density-temperature operating space with contours of auxiliary power in MW×10<sup>2</sup>.

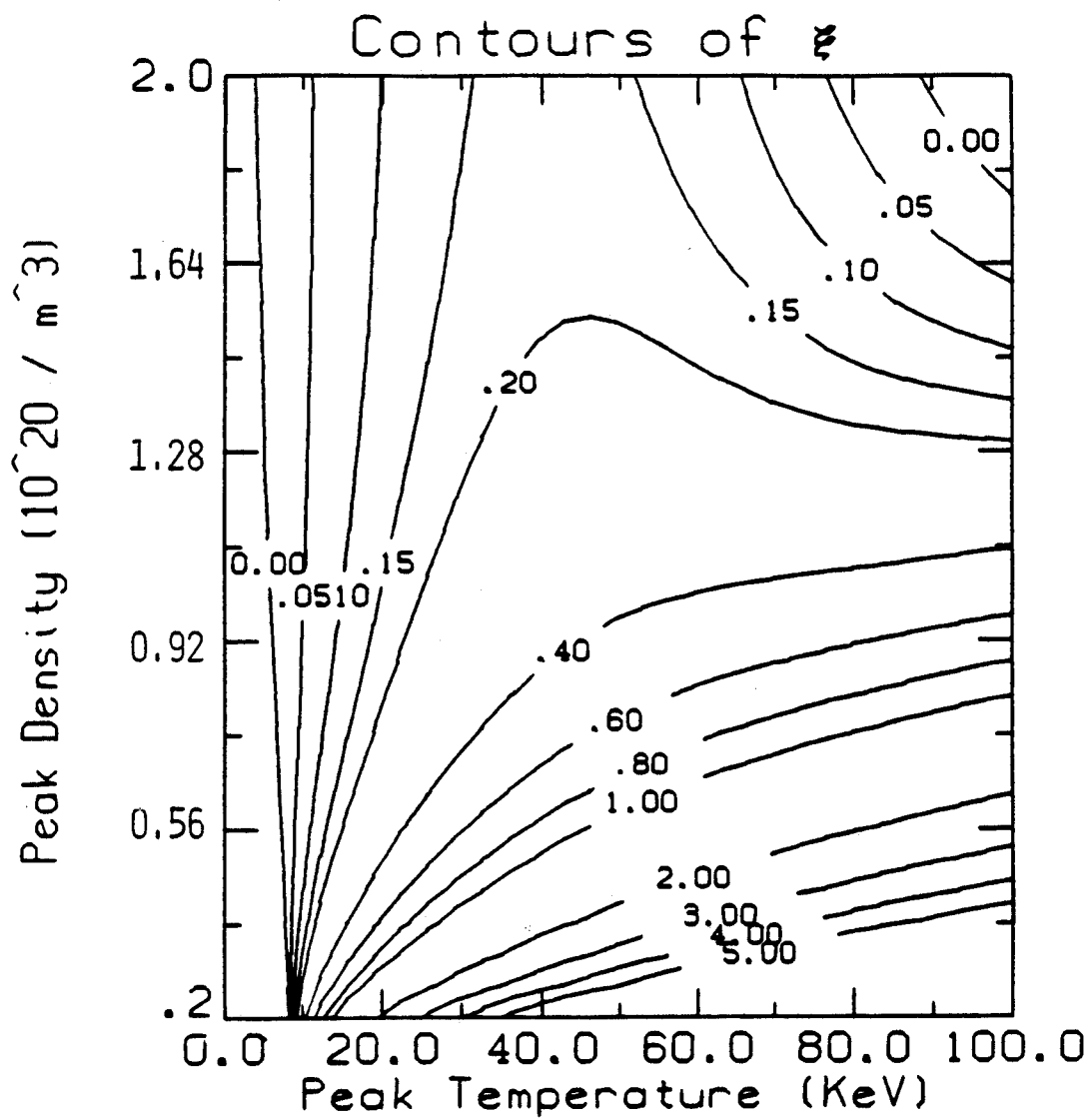


Figure 9: D-<sup>3</sup>He reactor contours of constant  $\xi$  (cf. Eq. 45) for D-T fusion. The  $P_{ICRF}$  values needed in evaluating  $\xi$  are taken from Fig. 8 at each value of density and temperature.

## 4 Dynamic Issues

A real plasma will experience temperature perturbations away from steady state which need to be stabilized in order to achieve the optimum performance required by a fusion reactor. In order to model this scenario, a time dependent plasma transport model is considered. The time dependent 0-D transport model (Eq. 7) can be used to analyse the global dynamic behavior of the plasma. For subignited plasmas, one method for stabilizing temperature fluctuations is by active auxiliary power modulation. Such a method has been considered in the past [12][13][14] [15][16][17] [18] finding that it can be used effectively to control both positive and negative temperature fluctuations.

As demonstrated in reference [15] the delay time  $\tau_d$  associated with the feedback system of a burn control scheme based on auxiliary power modulation is closely linked to the behavior of the complete control scheme. In the present analysis the work presented in [15] is expanded to include the effects of the energy transfer between the ICRF heated tail ions and the background plasma.

In an ICRF heated plasma the distribution tail of the resonant (heated) ions is raised thereby increasing the effective temperature of the heated species. When the ICRF power is shut-off, or when the amount of ICRF power supplied to the plasma changes, it takes a finite amount of time for the distribution function to achieve a new equilibrium. The new equilibrium is achieved by collisional equilibration among the plasma species. A full Fokker Plank simulation of Eq. (29) including fast alpha particle slowing down is possible but here we prefer to give a simplified analysis of a two component plasma. The background species (denoted by  $\beta$ ) is characterized by a Maxwellian distribution function with temperature  $T_\beta$ , and the hot test particles (denoted by  $\alpha$ ) are characterized by “temperature”  $T_\alpha$ . In such a plasma, the rate of change for the temperature of species  $\alpha$  is given in [19] as

$$\frac{dT_\alpha}{dT} = \frac{1}{\tau_\xi^{\alpha/\beta}} (T_\beta - T_\alpha), \quad (18)$$

where  $\tau_\xi^{\alpha/\beta}$  is the equipartition time for the temperature,

$$\tau_\xi^{\alpha/\beta} = \frac{3}{8\sqrt{2}\sqrt{\pi}} \frac{(m_\alpha T_\beta + m_\beta T_\alpha)^{3/2}}{\sqrt{m_\beta m_\alpha} Z_\alpha^2 Z_\beta^2 n_\beta \ln \Lambda_{\alpha/\beta}}. \quad (19)$$

Here  $m_j$ ,  $Z_j$ ,  $T_j$ , and  $n_j$  correspond to the mass, charge, temperature, and density of the  $j^{\text{th}}$  species. In MKS units, for the temperature given in keV and the density in units of  $10^{20}/\text{m}^3$  Eq. 19 becomes

$$\tau_\xi^{\alpha/\beta} = 5.5 \times 10^{10} \frac{(m_\alpha T_\beta + m_\beta T_\alpha)^{3/2}}{\sqrt{m_\beta m_\alpha} Z_\alpha^2 Z_\beta^2 n_\beta \ln \Lambda_{\alpha/\beta}}. \quad (20)$$

## 4.1 The complete 0-D time dependent model

The relation which describes the volume averaged (0-D) evolution of the plasma temperature is given by Eq. (7). For a given heating power, the characteristic time associated with the evolution of the global temperature is proportional to the energy confinement time  $\tau_E$ . [15] The next step in developing the complete 0-D transport model is to characterize the feedback system required for performing burn control simulations, and to determine the various delay times and characteristic times associated with the system. In reference [15] the equations characterizing an auxiliary power burn control system are derived. These equations are: the energy balance equation, the equation characterizing the effect of fusion particle thermalization, and the equation describing the feedback system behavior.

$$\frac{dT}{dt} = \mathcal{G}(T, n, P_\alpha(n, T), P_{aux}(T_d)) \quad (21)$$

$$\frac{dP_\alpha}{dt} = \frac{1}{\tau_\alpha} [Q_\alpha(n, T) - P_\alpha(n, T)] \quad (22)$$

$$\frac{dT_d}{dt} = \frac{1}{\tau_d} [T - T_d]. \quad (23)$$

where the equation describing the evolution of plasma particle density has been omitted. Equation (21) corresponds to the energy balance Eq. (7).  $\mathcal{G}$  is a function of the plasma temperature ( $T$ ), the density ( $n$ ), the fusion power absorbed by the plasma at time  $t$  ( $P_\alpha$ ), and the auxiliary power supplied to the plasma at time  $t$  ( $P_{aux}(T_d)$ ). Note that  $T$  is the temperature of the plasma at time  $t$  and  $T_d$  is the temperature that the feedback system responds to at time  $t$ . (This concept is briefly elucidated in Appendix B). Equation (22) represents the effect of finite thermalization time for the fusion products (i.e. alpha particles in D-T fusion).  $Q_\alpha$  represents the amount of fusion power produced at time  $t$ ,  $P_\alpha$  is the amount of fusion power absorbed by the bulk plasma at time  $t$ , and  $\tau_\alpha$  corresponds to the fusion particle thermalization time. Equation (23) models the feedback system which is characterized by a delay time  $\tau_d$ .

Equations (21,22,23), along with the equations characterizing the density evolution, have been used in [15] for modeling the burn control system of the Compact Ignition Tokamak. There it was found that the feedback delay time  $\tau_d$  is strongly related to the performance of the overall control system. Depending on the value of  $\tau_d$  the feedback system can be underdamped or overdamped. An overdamped system is characterized by small  $\tau_d$  ( $\leq 1/10$  sec). As  $\tau_d$  increases the system becomes underdamped and the smallest perturbations may result in global thermal instability particularly when  $\tau_d$  becomes greater than 1-2 seconds.

For the problem at hand a simple modification must be made to the model presented by Eqs. (21-23) in order to include the effect of distribution function modification due to ICRF heating. The basic principle is that the problem is now characterized by another delay time which is a function of the change induced to the distribution function due to ICRF heating. This time delay is labeled  $\tau_\xi$  and is given by Eq. 20.

When the plasma is heated by ICRF waves the energy is stored in the plasma due to the change of the distribution function which has an effective

temperature  $T$ . As the heating is cut off the characteristic energy thermalization time of the heated ions with the background plasma is given by  $\tau_\xi$ . By taking into account this phenomenon the complete burn control model is given by

$$\frac{dT}{dt} = \mathcal{G}(T, n, P_\alpha(n, T), P_{aux}(T)) \quad (24)$$

$$\frac{dP_\alpha}{dt} = \frac{1}{\tau_\alpha} [Q_\alpha(n, T) - P_\alpha(n, T)] \quad (25)$$

$$\frac{dT_d}{dt} = \frac{1}{\tau_d} [T - T_d] \quad (26)$$

$$\frac{dP_{aux}}{dt} = \frac{1}{\tau_\xi} (Q_{aux}(T_d) - P_{aux}(T)) \quad (27)$$

Here,  $Q_{aux}$  is the amount of auxiliary power deposited in the plasma at time  $t$  and  $P_{aux}$  is the amount of auxiliary power transferred to the bulk plasma at time  $t$ .

## 4.2 Time dependent simulations

Using Eqs. 24-27 the dynamic behavior of a D-<sup>3</sup>He tokamak plasma is investigated under various temperature perturbations and for different values of the system characteristic delay times  $\tau_d$  and  $\tau_\xi$ .

The equilibrium about which the dynamic behavior is to be investigated is chosen from the operating space of the D-<sup>3</sup>He reactor shown in Fig. 8. In particular the chosen operating point is: peak electron density  $1.0 \times 10^{20}/\text{m}^3$  and peak electron temperature 60 keV. At this operating point, and for the case where the distribution functions of both the deuterium and <sup>3</sup>He ions are represented by Maxwellians, steady state operation is achieved with 36 MW of auxiliary power. By incorporating the change in the distribution function due to ICRF heating the required auxiliary power for steady state operation at the the same point is reduced to 26 MW.

Equation (27) requires the characterization of the function  $Q_{aux}(T)$  which represents the feedback system response. In this analysis the relation of auxiliary power to temperature is chosen to be

$$Q_{aux}(T) = \begin{cases} Q_{max} & T < T_1 \\ Q_{max} \left[ 1 - \left( \frac{T-T_1}{T_2-T_1} \right)^\lambda \right] & T_1 < T < T_2 \\ 0 & T > T_2 \end{cases} \quad (28)$$

The above equation represents a proportional feedback law.  $Q_{max}$  is the maximum amount of auxiliary power available.  $T$  is the temperature which the system attempts to stabilize.  $T_1$  is a temperature below which the control system supplies the maximum amount of auxiliary power  $Q_{max}$  and  $T_2$  is a temperature above which the the auxiliary power is zero. The exponent  $\lambda$  represents the rate of change of auxiliary power with temperature. In the results presented below it is assumed that  $T_1 = 55$  keV,  $T_2 = 67$  keV,  $\lambda = 2$  and  $Q_{max} = 30$  MW.

As a base case the dynamic stabilization of a D-<sup>3</sup>He plasma, without the effect of ICRF heating on distribution function modification “no  $\xi$  effect”, is considered first. Figure 10 shows the evolution of the global plasma temperature after a 10% temperature perturbation at time  $t = 0.5$  sec. The feedback system responds by reducing the auxiliary power supplied to the plasma with a resulting decrease in temperature. The amount of auxiliary power supplied by the feedback system,  $Q_{aux}$ , is equal to the amount of auxiliary power transferred to the bulk plasma since the effect of heating on the distribution function is not considered. In this situation the plasma temperature equilibrates within one second of the disturbance.

In order to investigate the effect of ICRF heating on the plasma dynamics, as presented by Eqs. 24-27, the evolution of the plasma temperature following a 10% temperature perturbation is investigated under various assumptions for the characteristic time  $\tau_\xi$ .

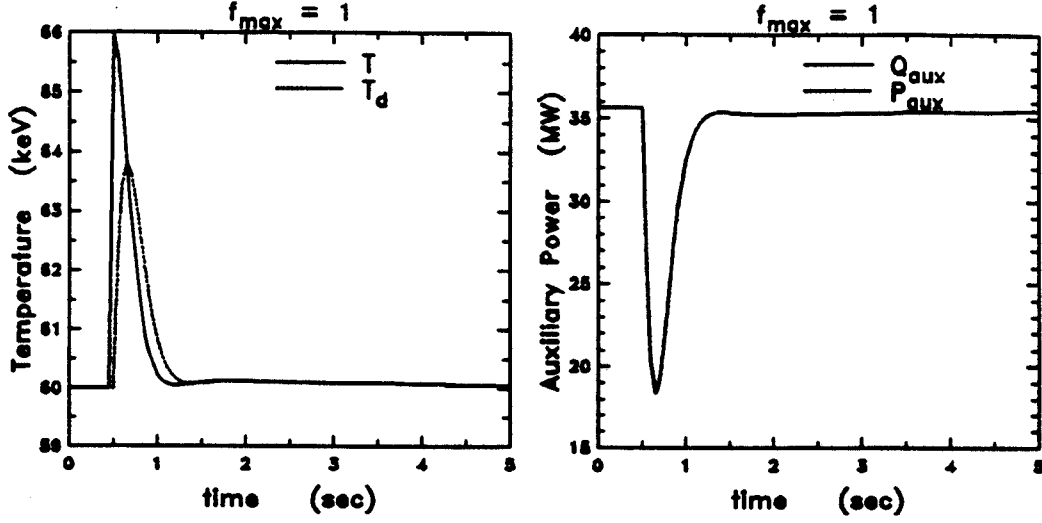


Figure 10: Stabilization of a 10% positive temperature deviation (left) with the aide of auxiliary power (right) for a D-<sup>3</sup>He reactor plasma. The effect of ICRF heating on distribution function modification is not considered. The system is characterized by a feedback delay time  $\tau_d = 0.1$  seconds.

First, for  $\tau_\xi = 0.1$  seconds and for  $\tau_d = 0.1$  seconds the temperature and auxiliary power evolution following a perturbation is shown in Fig. 11. Note that by considering the  $\xi$  effect due to ICRF the system becomes underdamped as it is apparent by the overshooting and eventual stabilization of the system within two seconds of the disturbance. By increasing the characteristic time  $\tau_\xi$  to 0.5 seconds the system is further underdamped and it is eventually stabilized within 5 seconds from the disturbance (see Fig. 12).

The characteristic time  $\tau_\xi$  is a function of the plasma parameters as given by Eq. (20). At the equilibrium point (i.e. at  $T_{e0} = 60$  keV and  $n_{e0} = 1.0/\text{m}^3$ ) Eq. (20) gives  $\tau_\xi = 0.72$  seconds. For  $\tau_\xi$  given by Eq. (20) the evolution of the plasma temperature following a 10% positive and negative temperature perturbation is shown on Fig. 13. Note that the perturbation is stabilized after substantial oscillations about the equilibrium which indicates that the system is underdamped.

In the example presented here the longest time constant in the problem is the energy confinement time  $\tau_E$ . At the equilibrium of interest the energy



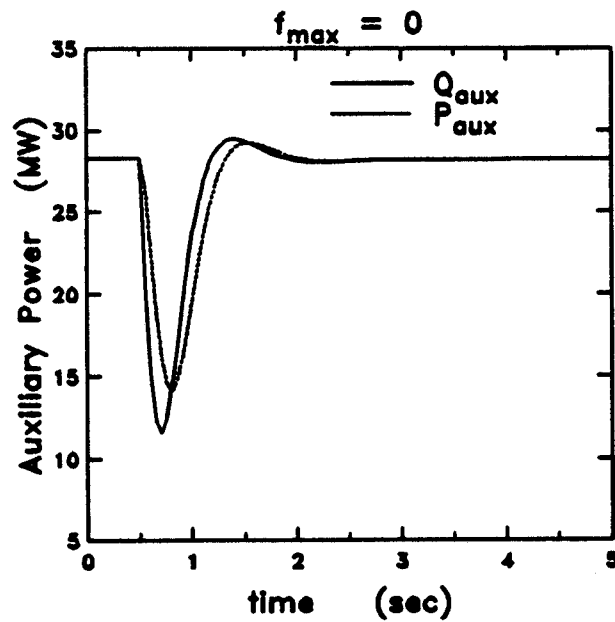
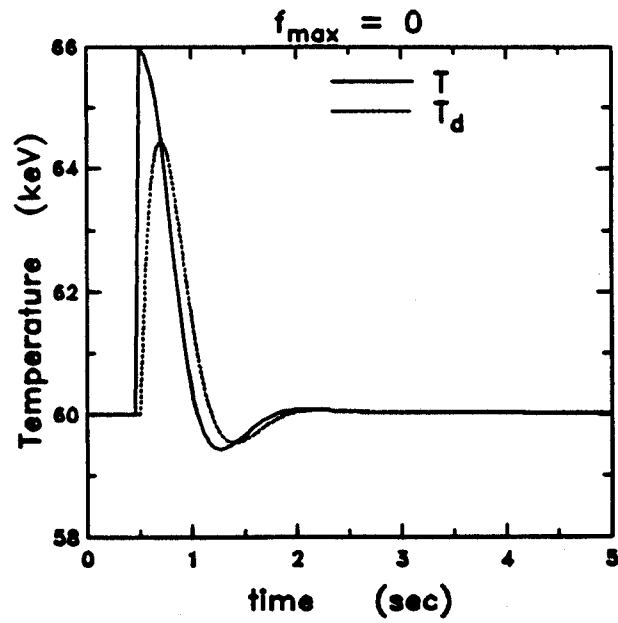


Figure 11: The stabilization of a 10% positive temperature deviation with the aide of auxiliary power for a D-<sup>3</sup>He reactor plasma. The system is characterized by a feedback delay time  $\tau_d = 0.1$  seconds and by a tail relaxation delay time  $\tau_\xi$  which in this plot is set equal to 0.1 seconds. The top figure shows the temperature evolution and the bottom figure represents the evolution in the auxiliary power.

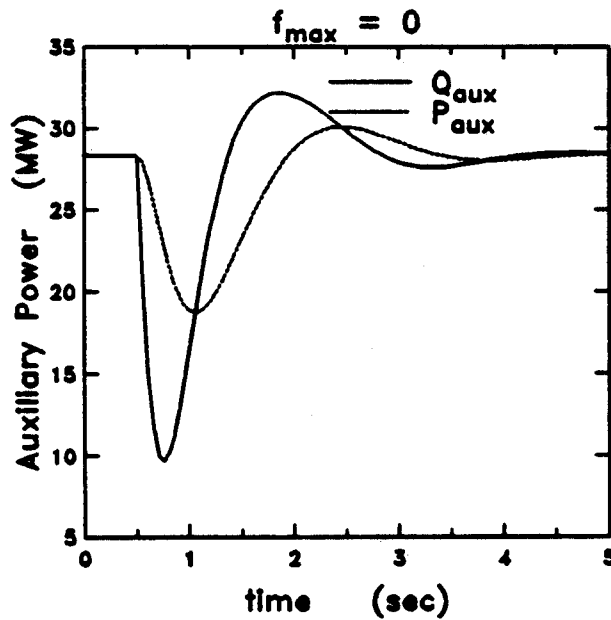
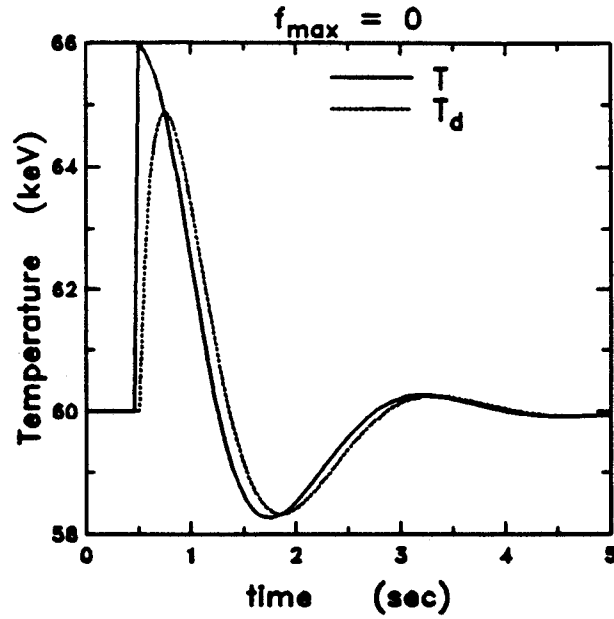


Figure 12: The stabilization of a 10% positive temperature deviation with the aid of auxiliary power for a D-<sup>3</sup>He reactor plasma. The system is characterized by a feedback delay time  $\tau_d = 0.1$  seconds and by a tail relaxation delay time  $\tau_\ell$  which in this plot is set equal to 0.5 seconds. The top figure shows the temperature evolution and the bottom figure represents the evolution in the auxiliary power.

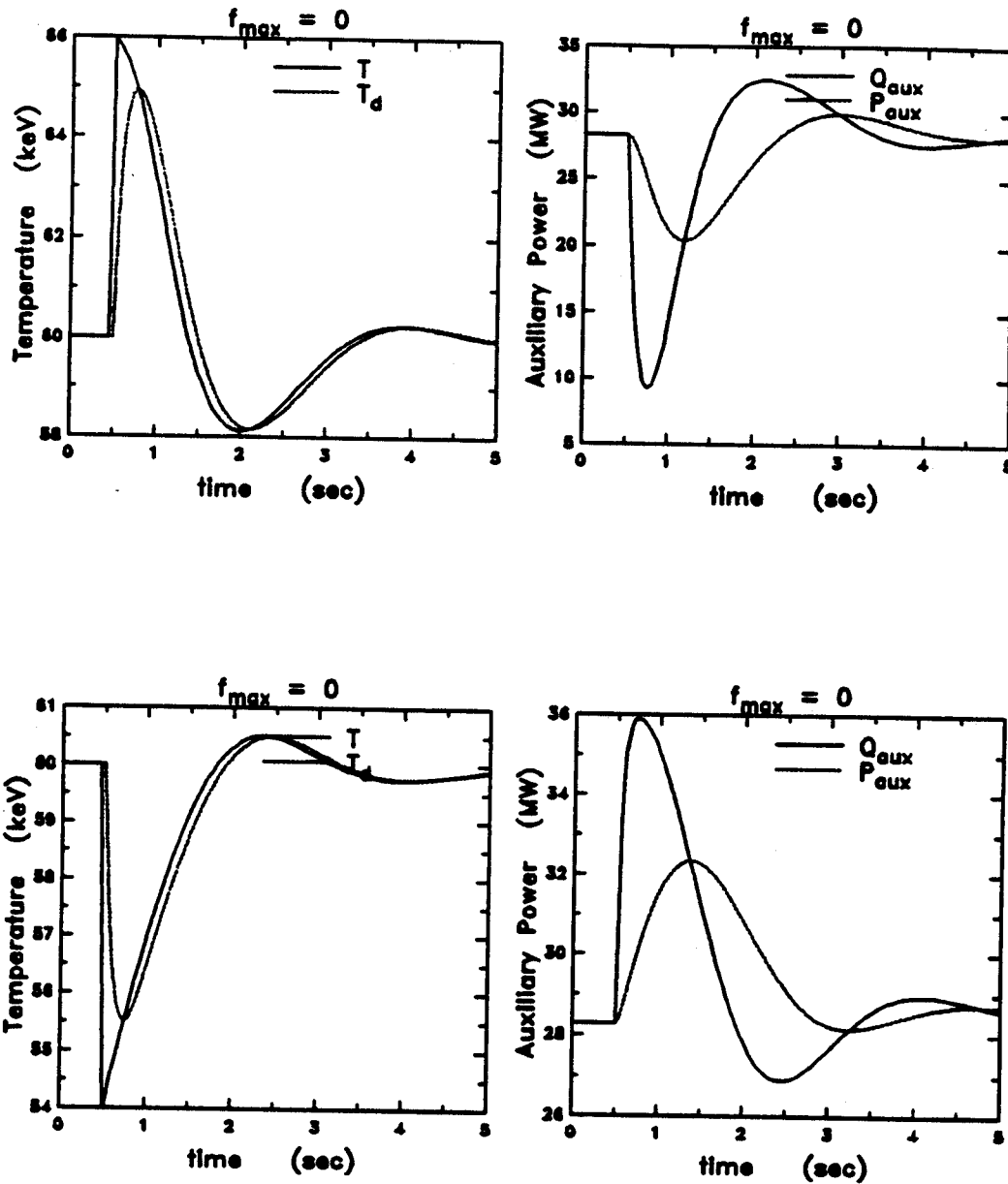


Figure 13: A plot indicating the stabilization of a 10% positive (top figure) and negative (bottom figure) temperature deviation with the aide of auxiliary power for a D-<sup>3</sup>He reactor plasma. The system is characterized by a feedback delay time  $\tau_d = 0.1$  seconds and by a tail relaxation delay time  $\tau_t$  which in this plot is given by Eq. 20.

confinement time is 11 seconds for ITER89P scaling with an H-mode factor of 4. For  $\tau_\xi = \tau_E$  a simulation of the control is shown on Fig. 14. In this situation the system is severely underdamped and it takes a long time for the system to return to equilibrium.

The phenomenological variations of  $\tau_\xi$  in the range  $\tau_d \leq \tau_\xi \leq \tau_E$  assumed in our time response studies are intended to show the consequences of fuel ion tail heating without addressing the underlying causes for a given value of  $\tau_\xi$ . In actual burning plasmas, the tail equilibration will be more complicated than given in Eqs. (20)-(18). The tail ion distribution can be modelled more accurately using a bounce averaged rf Fokker-Planck code. In addition to collisional temperature equilibration the **effective** relaxation time  $\tau_\xi$  may be determined by fluctuation driven energy exchange and by less than perfect coupling of the fast fusion products to the bulk plasma due to anomalous spatial losses during slowing down.[9] This coupling efficiency  $\eta_f$  (where  $f$  denotes fast ions including fusion products) is a quantity of great interest since it determines the power balance of the burning plasma. When  $\eta_f < 1$ , substantially more auxiliary power may be needed to produce the same ignition margin  $n\tau T$ . At present, first theoretical models of  $\eta_f$  are forthcoming [9, 20] but a predictive capability for the performance of an engineering test reactor will require crucial comparisons with experiments. One can use the time dependent modelling of the response to a temperature perturbation developed above to shed light on the magnitude of  $\tau_\alpha$ ,  $\tau_\xi$  (cf. Eqs. (25)-(27) and the underlying physical mechanisms, by comparing the simulation results (such as Figs. 11-14) with experimental measurements in a manner reminiscent of heat pulse propagation studies of the electron thermal conductivity  $\chi_e$  using the sawtooth crash or an applied local heat pulse at the  $q = 1$  surface.

## 5 Summary and Conclusions

When feedback control of the auxiliary heating power  $P_{aux}$  is used to provide thermal stability for an underignited fusion plasma, this heating (particularly ICRF minority heating) can produce an ion tail which affects the

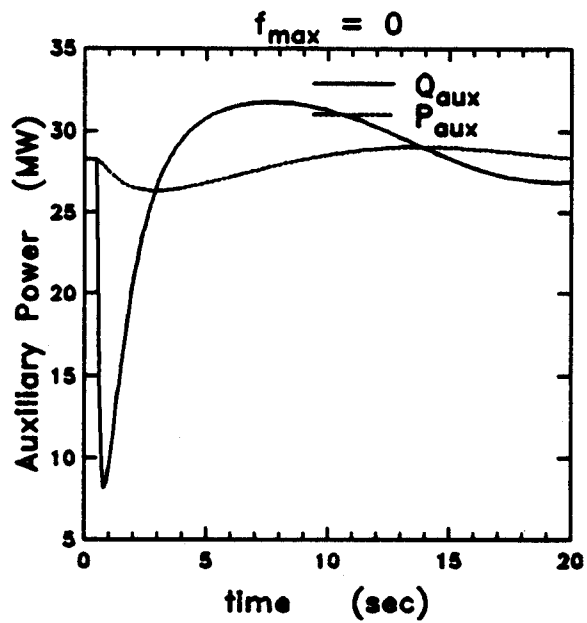
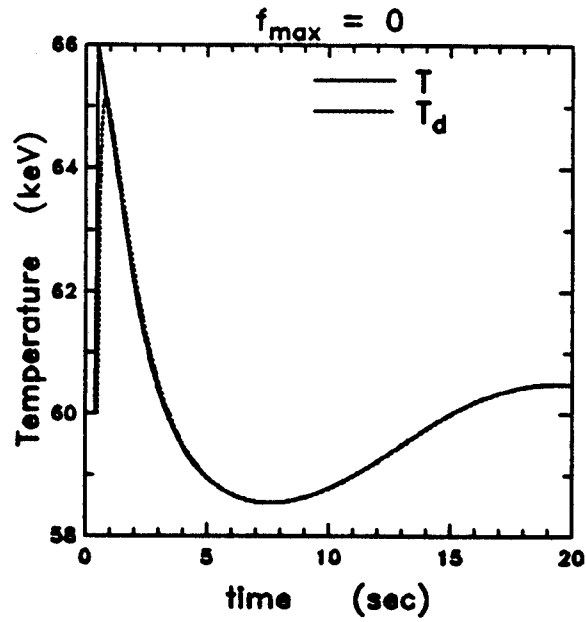


Figure 14: Stabilization of a 10% positive temperature deviation (top figure) with the aide of auxiliary power (bottom figure) for a D-<sup>3</sup>He reactor plasma. The system is characterized by a feedback delay time  $\tau_d = 0.1$  seconds and by a tail relaxation delay time  $\tau_\xi$  which in this plot is set equal to the energy confinement time  $\tau_E$ .

fusion reactivity and hence the dynamic behavior of the plasma operating point.

Using the Stix formula for the ion tail formation due to ICRF minority heating we find substantial tail formation, i.e., the Stix parameter  $\xi$  (cf. Eq. (2)) is  $\leq 1$  for typical operating points ITER, and  $\xi \geq 1$  in a D-<sup>3</sup>He reactor. For typical ITER and D-<sup>3</sup>He plasmas the above mentioned values of the Stix parameter result in enhancement of the fusion reactivity by a factor of 1.5 to 3. This reactivity enhancement corresponds to a reduction of the required auxiliary power by 20 - 25 %.

Extending this approach to the time dependent volume averaged power balance we have presented a dynamic feedback model based on controlling  $P_{aux}$  with a time delay  $\tau_d$  (reflecting not only the feedback circuit response but also the finite response time needed for a sudden adjustment of the heating power source). In addition to  $\tau_d$  the model (Eqs. 24-27) depends on the effective fusion power thermalization time  $\tau_\alpha$  (which may be affected by anomalous fast  $\alpha$  diffusion losses) and the effective tail ion thermalization time  $\tau_\xi$  (similarly affected by classical and possibly anomalous processes). Increasing  $\tau_\xi/\tau_d$  increases the phase lag between the power  $Q_{aux}$  applied to the plasma and the power  $P_{aux}$  absorbed by the plasma, at a given time  $t$ , leading to an increasingly underdamped behavior of  $P_{aux}$  as well as the plasma temperature  $T$ . For  $\tau_\xi = \tau_E$ , the damping time of these oscillations is several times  $\tau_E$  in the D-<sup>3</sup>He reactor used here to demonstrate the effect.

Temperature excursions and the ensuing oscillations induce fluctuations in fusion power which may affect the fatigue characteristics of the mechanical components surrounding the plasma. In order to evaluate the magnitude of this effect a comparison between the frequency of the oscillations and the time constant which introduces adverse thermal cycling effects must be made.

Besides the consequences of these oscillations on the operating characteristics, the shape of the temperature excursions can be used to reveal and analyze the physical features of the underlying anomalous transport mechanisms determining  $\tau_\alpha$  and  $\tau_\xi$  which need to be understood to predict the burning plasma performance.

## **Acknowledgments**

The authors would like to thank Professor Jeff Freidberg for useful discussions during the preparation of this paper. This work was sponsored by U. S. DoE grant DE-FG02-91ER-54109.

## Appendix A: Theory of Tail Formation due to ICRF Heating

The bounce averaged Fokker-Plank equation is given by

$$\frac{\partial \langle f \rangle}{\partial t} = \frac{1}{\tau_B} \int [\mathcal{C}(f) + \mathcal{Q}(f)] \frac{dl}{|v_{||}|} \quad (29)$$

where  $\mathcal{C}$  corresponds to the local collision operator and  $\mathcal{Q}$  represents the local quasi-linear diffusion operator due to ICRF heating.  $\tau_B$  is the particle bounce period and is given by  $\tau_B = \int dl/|v_{||}|$  and  $\langle \cdot \rangle$  represents the bounce averaging operator. Eq. 29 can be written as:

$$\left\langle \frac{\partial f}{\partial t} \right\rangle = \langle \mathcal{C}(f) \rangle + \langle \mathcal{Q}(f) \rangle. \quad (30)$$

The bounce averaged collision operator,  $\mathcal{C}$ , may be written as

$$\langle \mathcal{C}(f) \rangle = \left\langle \frac{\partial}{\partial v} \Gamma(f) \right\rangle \quad (31)$$

where  $\Gamma$  is the flow in velocity space which, if pitch angle scattering and slowing down of fusion products is neglected, is simply

$$\Gamma = \sum_j \lambda_j A_j(v) \frac{1}{v^2} \left[ \frac{v_j^2}{2v} \frac{\partial f}{\partial v} + \frac{m}{m_j} f \right] \quad (32)$$

with the subscript  $j$  representing the background plasma species.  $m$  is the mass of the minority ion. The parameters  $\lambda_j$  and  $A_j$  are given by

$$\lambda_j = \frac{4\pi e^4 Z^2 Z_j^2 n_j \ln \Lambda}{m^2} \quad (33)$$

$$A_j = \frac{2}{\sqrt{\pi}} \int_0^{v/v_j} \sqrt{x} \exp(-x) dx \quad (34)$$

$$\simeq \frac{2/(3\sqrt{\pi})(v/v_j)}{1 + 4/(3\sqrt{\pi})(v/v_j)^3} \quad (35)$$



The quasi-linear operator  $\mathcal{Q}$  is given by

$$\mathcal{Q}(f) = \frac{\partial}{\partial v} \mathcal{D} \frac{\partial f}{\partial v} \quad (36)$$

The diffusion coefficient  $\mathcal{D}$  is given in reference [21], and upon bounce averaging it becomes

$$\mathcal{D} = \frac{1}{\tau_B} \frac{2}{3m} \langle \delta E_{\perp} \rangle \quad (37)$$

where  $\delta E_{\perp}$  is the change in particle energy due to its interaction with the wave. In terms of the ICRF absorbed power density  $\langle P \rangle$  the diffusion coefficient  $\mathcal{D}$  can be expressed as

$$\mathcal{D} = \frac{\langle P \rangle}{3 n m} \quad (38)$$

where  $n$  and  $m$  are the density and mass of the resonating (heated) particles.

Finally by substituting Eqs. 31 and 36 into Eq. 30 and dropping the bounce average operator  $\langle \rangle$ , the isotropic part of the Fokker-Plank equation becomes

$$\frac{\partial f}{\partial t} = \frac{\partial}{\partial v} \left[ \sum_j \lambda_j A_j(v) \frac{1}{v^2} \left( \frac{v_j^2}{2v} \frac{\partial f}{\partial v} + \frac{m}{m_j} f \right) + \mathcal{D} \frac{\partial f}{\partial v} \right] \quad (39)$$

In steady state ( $\partial f / \partial t = 0$ ) Eq. 39 is integrated twice with the result

$$\ln f(v) = - \int_0^v \frac{\sum_j \lambda_j A_j m / m_j}{\sum_j \lambda_j A_j v_j / (2v) + \mathcal{D} v^2} dv \quad (40)$$

With further algebraic manipulation of the above integral, the velocity distribution function of the resonant ions can be written as

$$f(v) = n \left( \frac{m}{2\pi T_e} \right)^{3/2} \exp \left[ - \frac{mv^2}{2T_e} \mathcal{F}(\xi) \right], \quad (41)$$

which is a Maxwellian modified by the function  $\mathcal{F}$ , where  $\mathcal{F}$  is given by [2]

$$\mathcal{F} = \frac{1}{1 + \xi} \left[ 1 + \frac{R_j(T_e - T_j + \xi T_e)}{T_j(1 + R_j + \xi)} H(E/E_j) \right] \quad (42)$$

In the above equation  $T_e$  the electron temperature and  $T_j$  the temperature of the background ions.  $\xi$  represents the effect of wave heating on the shape of the distribution function of the resonant ions and is given by

$$\xi = \mathcal{D} \frac{m^2 v_e}{2/(3\sqrt{\pi}) 4\pi n_3 \epsilon^4 Z^2 \ln \Lambda} \quad (43)$$

which according to Eq. 38 becomes

$$\xi = \frac{m \langle P \rangle}{8\sqrt{\pi} n_e n Z^2 e^4 \ln \Lambda} \left( \frac{2T_e}{m_e} \right)^{1/2} \quad (44)$$

Here,  $\langle P \rangle$  represents the ICRF heating power per unit volume delivered to the resonant ions,  $Z$  is the charge of the resonant ions. With the temperature  $T_e$  given in keV and the densities  $n_e$ ,  $n$  in units of  $10^{20}/\text{m}^3$  Eq. 44 becomes

$$\xi = 1.68 \times 10^6 \frac{m \langle P \rangle}{n_e n Z^2 \ln \Lambda} \left( \frac{2T_e}{m_e} \right)^{1/2} \quad (45)$$

The parameters  $R_j$ ,  $E_j$  and  $H$  in Eq. 42 are given by

$$R_j = \frac{n_j Z_j^2}{n_e} \left( \frac{m_j T_e}{m_e T_j} \right)^{1/2} \quad (46)$$

$$E_j = \frac{m}{m_j} T_j \left[ \frac{3\sqrt{\pi}(1 + R_j + \xi)}{4(1 + \xi)} \right]^{2/3} \quad (47)$$

$$H(x) = \frac{1}{x} \int_0^x \frac{du}{1 + u^{3/2}} \quad (48)$$

## Appendix B: A Simple Feedback Model

The question is how to choose a temporal evolution for the applied auxiliary heating power  $P_{aux} = P_{aux}(t)$  such that a spontaneous temperature excursion  $\Delta T$  introduced at  $t = 0^+$  leads to a damped oscillation of the plasma temperature. A simple choice is,

$$\frac{dT}{dt} = S - P_{aux}(T_d(t)), \quad (49)$$

where  $S$  denotes all other power sources and sinks. In equilibrium,

$$0 = S + P_{aux}(T_d = 0). \quad (50)$$

The “delayed temperature”  $T_d$  is chosen to obey

$$\frac{dT_d}{dt} = \frac{1}{\tau_d}(T - T_d) \quad (51)$$

where the constant delay time  $\tau_d$  is determined by the feedback mechanisms and the characteristic confinement and energy equilibration times of the plasma (which may, in reality, depend on  $T$ , themselves.)

We perform a perturbation analysis  $T = T_0 + \tilde{T}$ ,  $T_d = T_0 + \tilde{T}_d$ . The initial conditions at  $t = 0$  are:

$$T = T_d = T_0, \quad (52)$$

$$\tilde{T}_d(0) = 0, \quad \tilde{T}(0) = \Delta T, \quad (53)$$

where  $\Delta T$  is a sudden jump in temperature. Thus, for a small perturbation  $\Delta T$

$$P_{aux}(T_d) = P_{aux}(T_0) + \left. \frac{\partial P_{aux}}{\partial T_d} \right|_{T_0} (T_d - T_0) \quad (54)$$

so that

$$\frac{d\tilde{T}}{dt} = \frac{\partial P_{aux}}{\partial T_d} \Big|_{T_0} \tilde{T}_d, \quad (55)$$

and

$$\frac{d\tilde{T}}{dt} = \frac{1}{\tau_d} (\tilde{T} - \tilde{T}_d). \quad (56)$$

The feedback law, Eq. (55), is chosen such that  $\left(\frac{\partial P_{aux}}{\partial T_d}\right)_{T_0} < 0$ . The delayed response law, Eq. (56), is chosen to be linear. From Eqs. (55, 56),

$$\frac{d^2 \tilde{T}_e}{dt^2} + \frac{1}{\tau_d} \frac{d\tilde{T}_e}{dt} - \frac{1}{\tau_d} \left( \frac{\partial P_{aux}}{\partial T_d} \right)_{T_0} \tilde{T}_d = 0, \quad (57)$$

which is a damped harmonic oscillator, as desired, with oscillation frequency  $\left[ -\frac{1}{\tau_d} \left( \frac{\partial P_{aux}}{\partial T_d} \right)_{T_0} \right]^{1/2}$ . From Eq.(57) one can see that while  $T(t)$  jumps by  $\Delta T$  and then decays,  $T_d(t)$  first rises and, after a delay, decays also.

## References

- [1] J.M. Dawson, H.P. Furth, and F.H. Tunney. Production of Thermonuclear Power by Non-Maxwellian Ions in a Closed Magnetic Field Configuration. *Physical Review Letters*, 26:1156–1160, 1971.
- [2] T.H. Stix. Fast Wave Heating of a Two-Component Plasma. *Nuclear Fusion*. 15:737–754, 1975.
- [3] J. Kesner. Quasi-Linear Model for Ion Cyclotron Heating of Tokamaks and Mirrors. *Nuclear Fusion*. 18:781, 1978.
- [4] D. T. Blackfield and J.E. Scharer. Anisotropy and Tail Formation in ICRF-Heated Plasmas. *Nuclear Fusion*, 22:255, 1982.
- [5] J.E. Scharer, J. Jackquinot, P. Lallia, and F. Sand. Fokker-Plank Calculations for JET ICRF Heating Scenarios. *Nuclear Fusion*, 25:435, 1985.
- [6] R. W. Harvey, M. G. McCoy, G. D. Kerbel, and S. C. Chiu. ICRF Fusion Reactivity Enhancement in Tokamaks. *Nuclear Fusion*, 26:43, 1986.
- [7] G. Sadler and P van Belle. Fusion Cross Sections and Reactivities. Technical report, JET, 1989.
- [8] Asher Peres. Fusion Cross Sections and Thermonuclear Reaction Rates. *Journal of Applied Physics*, 50:5569–5571, 1979.
- [9] D.J. Sigmar and R. Gormley. Private Communication.
- [10] R.R. Parker et al. Progress in Tokamak Research at MIT. *Nuclear Fusion*, 25(3), 1985.
- [11] ITER Physics Design Guidelines. Technical Report 10, IAEA, Vienna, 1990. ITER documentation series.

- [12] L. Bromberg J. L. Fisher D. R. Cohn. Active burn control of ignited plasmas. *Nuclear Fusion*, 20(2), 1980.
- [13] E.A. Chaniotakis, J.P. Freidberg, and D.R. Cohn. Burn Control Using Auxiliary Power Modulation. APS-Plasma Physics Division, 1988. 13th Annual meeting.
- [14] E. A. Chaniotakis et al. CIT Burn Control Using Auxiliary Power Modulation. Technical Report PFC/RR-89-16, Massachusetts Institute of Technology, 1989.
- [15] E.A. Chaniotakis. *Ignition and Burn Control Characteristics of Thermonuclear Plasmas*. PhD thesis, Massachusetts Institute of Technology, 1990.
- [16] S.W. Haney, L.J. Perkins, and S.K. Ho. ITER Operating Point Selection and Burn Control. Technical report, Lawrence Livermore National Laboratory, 1989.
- [17] J. Mandrekas and W.M. Stacey. *Fusion Technology*, 19:57, 1991.
- [18] S.W. Haney, L.J. Perkins, J. Mandrekas, and W.M. Stacey. *Fusion Technology*, 18:606, 1990.
- [19] B. A. Trubnikov. *Particle Interactions in a Fully Ionized Plasma*, volume 1 of *Reviews of Plasma Physics*, pages 105–204. Consultants Bureau, New York, 1965.
- [20] D. Sigmar and Ya.I Kolesnichenko. *Nuclear Fusion*, 31(9), 1991.
- [21] C.F. Kennel and F. Engelmann. Velocity Space Diffusion from Weak Plasma Turbulence in a Magnetic Field. *Physics of Fluids*, 9:2377–2388, 1966.